

ON THE APPLICATION OF PIFS-SF AND $D_q(f(\alpha))$ TO DENDRITES ANALYSIS*

ZBIGNIEW J. GRZYWNA[†], MONIKA KRASOWSKA
AND JACEK STOLARCZYK

Department of Physical Chemistry and Technology of Polymers
Section of Physics and Applied Mathematics
Silesian University of Technology
Ks. M. Strzody 9, 44-100 Gliwice, Poland

(Received November 29, 2002)

Partitioned iterated function system-semifractals (PIFS-SF) and generalized fractal dimension (D_q) or $f(\alpha)$ formalism to analysis of amacrine dendrites of gold fish retina has been applied. The number of codes (PIFS-SF) has been used as a measure of dendrites complexity in comparison with $D_q/f(\alpha)$ behaviour. Some structure-functions (electrophysiological) correlations based on D_q negative part have also been shown.

PACS numbers: 61.43 Hr

1. Introduction

Dendrites are the most spectacular part of nerve cells or neurons. They extend from the cell body like antennae and provide an enlarged surface area to receive signals from the other nerve cells. Neurons of different functional classes show an astonishing variety in the patterns of branching of their dendrites where the most fundamental input–output adaptive processes take place [1, 2]. Quantitative, and effective, analytical description of dendrites structure is of great importance for interpreting experimental data, or in other words, for understanding the structure functions relationship. In the present work we will focus on dendrites of goldfish retina amacrine cells (see Fig. 1).

* Presented at the XV Marian Smoluchowski Symposium on Statistical Physics, Zakopane, Poland, September 7–12, 2002.

[†] e-mail: grzywna@zeus.polsl.gliwice.pl

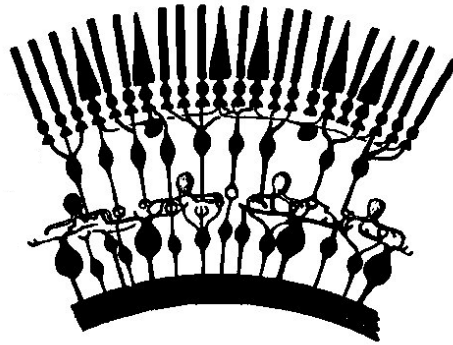


Fig. 1. The structure of retina. The amacrine cells form the middle layer.

Amacrine cells create an interneuronal branching system in retina. One of their basic functions is to participate in a course of combining information as well as presenting its image on the retina. The essence of visualisation process in retina consists of splitting the nerve signal into two ON and OFF paths, respectively (*cf.* [3]). In accordance with this pattern the inner plexiform layer (IPL), where amacrine cells receive their synaptic inputs, has been found to be organised broadly into two halves: OFF pathways are found in sublamina “a” (distal half), and ON signals are segregated to sublamina “b” (proximal half). This segregation is directly connected to the size and structure of the respective sublaminae. The problem is however to find the “right” measure of the structure in question which will help to show the structure-functions relation. Traditional approach of measuring the cross-sectional area of dendrites or the number of their branches gives no significant difference between sublaminae “a” and “b” [3]. In the present work we would like to show the application of the generalized dimension (D_q) and $f(\alpha)$ along the line showed only recently [4] as well as the possibility of using partial iterated function system — semifractals (PIFS-SF), tested, so far, only on analysis of the prototype structures [4,5].

2. Object of analysis





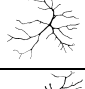
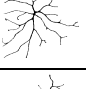

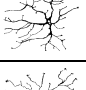

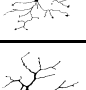

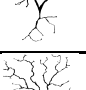
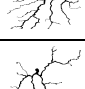
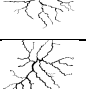


The object of our analysis were the amacrine cells of goldfish retina — a model of the central nervous system [1,3]. Retinae were isolated from dark-adapted goldfish (*Carassius auratus*).

The final set of cells is shown in Table I.

Note: the last letter indicates the sublamina a and b, other characters have no particular meaning but are used for discrimination.

TABLE I

Amacrine cells of goldfish retinae.

sublaminae a		sublaminae b	
a1a		a1b	
ab1a		ab1b	
ab2a		ab2b	
ab3a		ab3b	
ad3a		ad3b	
an4a		an4b	
b1a		b1b	
e2a		e2b	

3. Tools

Two different tools are going to be used in the present paper *i.e.* the generalized dimension (D_q) and its Legendre transform $f(\alpha)$, and the partitioned iterated function system-semifractals (PIFS-SF). Both are new in analysis of dendritic fields of amacrine cells. The necessity of new approach has been clearly shown by failure of a traditional one which was based on measuring the cross-sectional area of dendrites, or the number of their branches [8].

3.1. Fractal and generalized dimensions

Due to the well-established symmetry of dendrites in question, with soma centrally located, we have to alter the classical Box Counting Method (BCM) to Equal Area Box Counting Method (EABCM) while calculating d_F and

D_q . (see Table II)

$$d_F = \lim_{\varepsilon \rightarrow 0} \frac{\ln N(\varepsilon)}{\ln 1/\varepsilon}, \quad (1)$$

where $N(\varepsilon)$ — number of nonempty boxes needed to cover the set
 ε — the current size of the box

$$D_q = \frac{1}{q-1} \lim_{\varepsilon \rightarrow 0} \frac{\ln \sum_{i=1}^{N(\varepsilon)} P_i^q}{\ln \varepsilon}. \quad (2)$$

Results from five different methods *i.e.* IRRM (increasing radius and rings method) [6], BCM (box counting method) [6], IAM (increasing angle methods) [6], MRM (mass radius method) [7] and EABCM (equal-area box counting method) [3] have been used in fractal analysis of dendritic trees of amacrine cells. The studies have shown that different methods covered different aspects of the complex nature of investigated sets, especially if they are spatially oriented.

Properties of $D_q/f(\alpha)$ spectra needed for our analysis have been described in the previous paper [4].

3.2. PIFS-SF

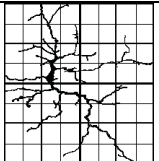
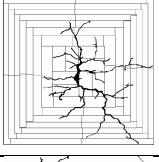
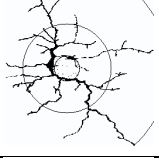
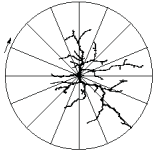
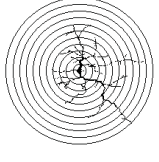
The technique of Partitioned Iterated Function System takes advantage of the image intrinsic self-similarities. Rather than being written as a matrix of points with given value (brightness/darkness), the image is treated as a set of linear contractive transforms of one fragment of itself into another.

The basic idea of encoding an image in terms of transforms comes from the work of Barnsley [10] on IFS. Since it is rather uncommon for any real object (image) to be composed of its own diminished copies, like in the original Barnsley's treatment, Jacquin [9] enhanced the concept by allowing parts of the image to be contracted copies of different parts. Indeed a branching section of the dendrite does not look like a whole dendrite, yet it may be very similar to other branching sections, possibly seen in different scale. In further development Grzywna *et al.* [5] adopted the notion of semifractals [11] so that not all transforms need to be contractive. Some of them may be scale-preserving (theoretically all but one, but in practice usually much less). It follows from another observation that parts of the image often resemble other parts of the same size. The encoding algorithm based on PIFS is widely used as an image compression tool, but compression issues are not subjects of present study.

The details of the technique are given elsewhere [5], we shall concentrate here on its application to dendrites. The image is partitioned into "range

TABLE II

Methods of calculation d_F and D_q .

BCM	
EABCM	
MRM	
IAM	
IRRM	

blocks” and each block is coded separately — for each block a matching “domain block” is searched in the image:

$$\mu = \bigcup_{i=1}^N \mu_{\lceil R_i}. \quad (3)$$

Each range block μ_{R_i} is itself coded by a transform τ or it is a union of smaller range blocks

$$\mu_{\lceil R_i} = \tau(\mu_{\lceil D_i}) \cup \bigcup_{j=1}^K \mu_{\lceil R_{i,j}}. \quad (4)$$

Repeating recursively such algorithm on the image of the dendrite shown in Fig. 2 (subimage ab1a) produces a sequence of partitions.

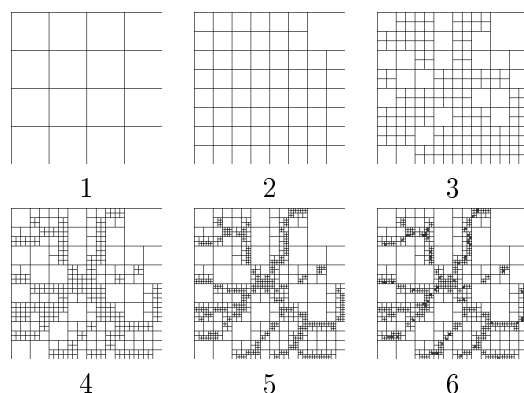


Fig. 2. Sequence of partitions given by Eqs. (3) and (4).

Set of codes calculated on each step of encoding (see Fig. 2) may be decoded to get a corresponding sequence of images with improving quality, shown in Fig. 3.

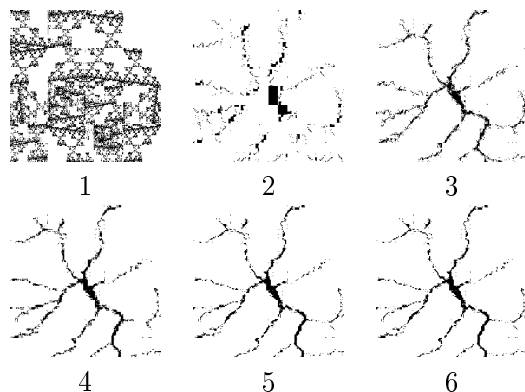


Fig. 3. Sequence of images corresponding to the sequence of partitions presented in Fig. 2.

The interesting feature of coding an object as a set of transforms is that no matter what the initial image looks like (it may even be noise) the decoding procedure quickly converges to the encoded object. Figure 4 shows first four steps of decoding and recovering the encoded image of a dendrite.

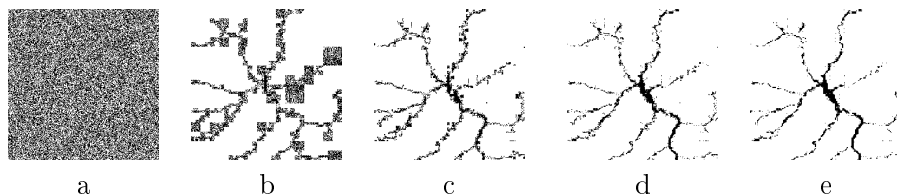


Fig. 4. Initial image (a) and four consecutive steps (b)–(e) of decoding procedure by application of PIFS-SF transforms.

4. Results and discussion

4.1. D_q

This paper shows five methods: IRRM, IAM, BCM, EABCM and MRM. IRRM determines d_F on the basis of scaling of the object's mass with its radius while IAM method uses scaling of the object's mass with an angle. Both methods can reveal iso/anisotropy of the object. The relation $\ln M(\varepsilon)$ versus $\ln \varepsilon$ shows whether:

- the mass of the object is homogeneously distributed along the radius (IRRM)(see Fig. 5(a));
- the number of branches and their thickness brings about a homogeneously distribution of a mass, independently of the direction (IAM) (see Fig. 5(b)).

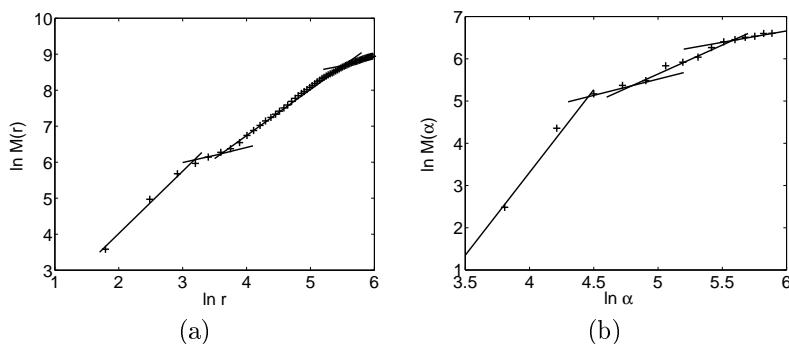


Fig. 5. Relation $\ln M(\varepsilon)$ versus $\ln \varepsilon$ for IRRM and IAM methods.

In case of anisotropic objects however the value of d_F is lowered. While covering the object by a grid of smaller and smaller size, the methods BCM and EABCM give information about self-similarity of the object. In the

BCM method it is a rectangular grid, which does not take into account the symmetry of the analysed object. The grid used in the method EABCM consists of rectangles of equal areas, arranged like rings around the geometric centre of an object. Results from fractal analysis by using BCM and EABCM methods are given in Tables III to VI. The method MRM [7] is based on analysing self-similarity according to 12 randomly chosen points of the objects and successive averaging of obtained results. Only two of five methods presented here can be applied for determination of D_q : BCM and EABCM. It is possible then to define a probability of finding a part of analysed object in a given element of a grid. For isotropic, regular objects for which a self-similarity does not depend either on a radius or on an angle, the values of d_F and D_q are the same (see Fig. 6).

TABLE III

Results from BCM method — part1.

cell	b1a	a1a	e2a	ab2a	ab1a	an4a	ab3a
$V_{\text{off}}(\text{mV})$	2.13	2.15	3.13	3.53	3.63	4.31	6.75
$D_{-\infty}$	2.20	2.04	1.88	2.04	1.93	1.97	2.00
D_{-3}	1.91	1.78	1.66	1.79	1.71	1.74	1.74
D_{-2}	1.83	1.70	1.60	1.71	1.65	1.68	1.67
D_{-1}	1.71	1.61	1.53	1.61	1.57	1.59	1.58
D_0	1.61	1.52	1.45	1.52	1.49	1.50	1.49
D_1	1.55	1.47	1.40	1.47	1.44	1.44	1.43
D_2	1.52	1.44	1.37	1.44	1.41	1.40	1.40
D_3	1.50	1.42	1.35	1.42	1.39	1.38	1.38
$D_{+\infty}$	1.40	1.31	1.25	1.28	1.24	1.29	1.28

TABLE IV

Results from BCM method — part2.

cell	ab1b	ab2b	a1b	b1b	e2b	ab3b	an4b
$V_{\text{on}}(\text{mV})$	1.50	2.09	2.25	2.44	3.31	5.25	6.19
$D_{-\infty}$	2.04	2.01	2.03	2.11	2.02	2.08	1.96
D_{-3}	1.79	1.77	1.80	1.85	1.78	1.84	1.72
D_{-2}	1.73	1.70	1.73	1.77	1.72	1.77	1.65
D_{-1}	1.64	1.61	1.64	1.67	1.64	1.68	1.57
D_0	1.57	1.53	1.56	1.58	1.56	1.59	1.49
D_1	1.52	1.48	1.51	1.53	1.51	1.53	1.44
D_2	1.49	1.45	1.48	1.50	1.48	1.49	1.40
D_3	1.47	1.43	1.46	1.48	1.46	1.47	1.38
$D_{+\infty}$	1.33	1.43	1.35	1.33	1.30	1.36	1.28

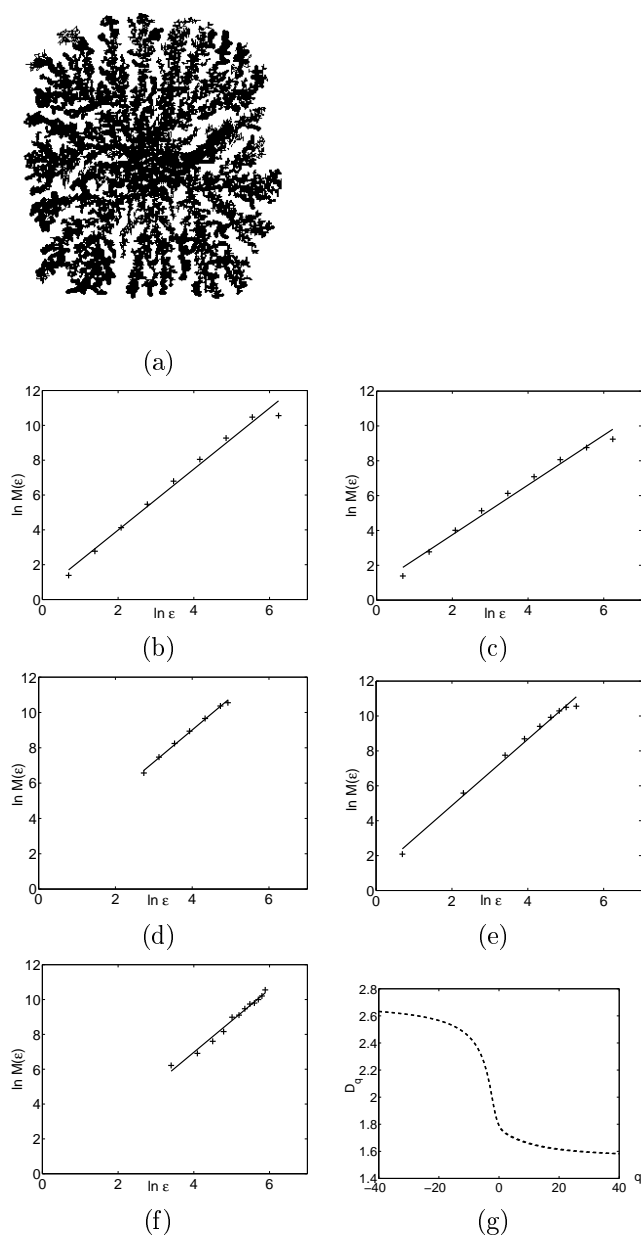


Fig. 6. DLA aggregate (a) and $\ln M(\epsilon)$ versus $\ln \epsilon$ for all methods (b)–(f) and D_q spectrum for BCM and EABCM methods (g).

TABLE V

Results from EABCM method — part1.

cell	b1a	a1a	e2a	ab2a	ab1a	an4a	ab3a
$V_{\text{off}}(\text{mV})$	2.13	2.15	3.13	3.53	3.63	4.31	6.75
$D_{-\infty}$	1.91	2.03	2.10	2.01	2.01	2.07	2.17
D_{-3}	1.67	1.71	1.78	1.75	1.76	1.81	1.88
D_{-2}	1.61	1.63	1.70	1.68	1.69	1.74	1.81
D_{-1}	1.54	1.56	1.60	1.61	1.63	1.67	1.72
D_0	1.45	1.48	1.50	1.53	1.55	1.57	1.63
D_1	1.43	1.45	1.47	1.51	1.52	1.50	1.60
D_2	1.42	1.42	1.41	1.47	1.48	1.42	1.58
D_3	1.21	1.36	1.33	1.35	1.41	1.32	1.36
$D_{+\infty}$	0.84	1.15	1.10	1.04	1.21	1.01	0.98

TABLE VI

Results from EABCM method — part2.

cell	ab1b	ab2b	a1b	b1b	e2b	ab3b	an4b
$V_{\text{on}}(\text{mV})$	1.50	2.09	2.25	2.44	3.31	5.25	6.19
$D_{-\infty}$	2.11	2.22	2.22	2.21	2.24	2.37	2.46
D_{-3}	1.74	1.78	1.83	1.84	1.83	1.95	2.04
D_{-2}	1.63	1.66	1.72	1.73	1.72	1.82	1.91
D_{-1}	1.48	1.53	1.56	1.57	1.58	1.67	1.74
D_0	1.39	1.45	1.47	1.47	1.49	1.57	1.61
D_1	1.36	1.44	1.40	1.46	1.46	1.54	1.58
D_2	1.35	1.42	1.34	1.40	1.45	1.52	1.54
D_3	1.22	1.25	1.29	1.30	1.33	1.31	1.37
$D_{+\infty}$	0.97	0.94	1.02	1.08	1.13	1.00	1.06

Generalized fractal dimension analysis (obtain by EABCM method) suggested that a consistent relationship exists between the fractal dimension D_{-2} , D_{-1} and D_0 in two functional domains of the IPL, *i.e.* sublamina a *vs.* b [3]. No correlation could be determined for electrophysiological properties and D_q by BCM method; correlation coefficient for d_F and V_{on} is -0.39 , and d_F while V_{off} equals -0.44 .

4.2. PIFS

The most important parameter that may be obtained from analysis by PIFS-SF is a number of codes. It allows for direct comparison between various analysed dendrites, both in terms of absolute and relative numbers.

The absolute numbers of codes for dendrites shown in Table I are given in Table VII.

TABLE VII

Number of codes needed to encode dendrites listed in Table I with the same accuracy.

sublaminae a		sublaminae b	
name	No. of codes	name	No. of codes
e2a	430	an4b	1225
ab1a	1669	ab2b	1990
ab3a	1672	e2b	2014
an4a	1687	a1b	2269
a1a	1999	ab1b	2302
ab2a	2002	ab3b	2506
b1a	3064	b1b	2680

These results may be easily compared with fractal dimension calculated by methods given in section 3.1. Correlation coefficients between the number of codes and box counting fractal dimension are listed in Table VIII.

TABLE VIII

Correlation coefficients between number of PIFS-SF codes and fractal dimension calculated by box-counting. “a” refers to sublaminae a, “b” to sublaminae b, respectively. “ab” stands for the whole set of dendrites.

$\rho(\text{PIFS}, d_F)$	value
ρ_a	0.952
ρ_b	0.950
ρ_{ab}	0.935

It appears that the correlation between results from these two techniques of analysis is very good, disrespective of the particular type of dendrites in question. More insight may be obtained by inspecting relative results (relative with respect to the highest value in each group, *i.e.* number of codes and fractal dimension). These values have been collected in Table IX.

The results given in Table IX show that PIFS-SF seems to be far more sensitive. Number of codes changes five-fold while the fractal dimension varies between dendrites only by about 10%. The difference stems from the partitions that both methods use to cover the image. While fractal dimension always uses rectangular lattice (see Fig. 7(a)), PIFS on each stage of encoding automatically adjusts itself to the image (Fig. 7(b)). Only relevant “blocks” are further divided and become encoded with better accuracy.

TABLE IX

Relative numbers of codes and fractal dimension for dendrites of amacrine cells shown in Table I.

sublaminae a			sublaminae b		
name	n/n_{\max}	$d_F/d_{F\max}$	name	n/n_{\max}	$d_F/d_{F\max}$
e2a	0.14	0.90	an4b	0.40	0.93
ab1a	0.54	0.93	ab2b	0.65	0.95
ab3a	0.55	0.93	e2b	0.66	0.97
an4a	0.55	0.93	a1b	0.74	0.97
a1a	0.66	0.94	ab1b	0.75	0.98
ab2a	0.66	0.94	ab3b	0.82	0.99
b1a	1.00	1.00	b1b	0.87	0.98

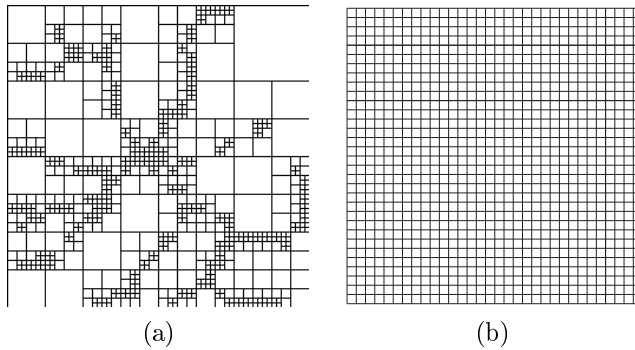


Fig. 7. Comparison of coverages used by box counting (a) and PIFS-SF (b).

Similarly to results for fractal analysis obtained by BCM method, the number of PIFS-SF codes weakly anticorrelates ($\rho(\text{PIFS}, V_{\text{off}}) = -0.48$, $\rho(\text{PIFS}, V_{\text{on}}) = -0.52$) with electrophysiological responses of the cells. This is an expected result, as d_F and the number of codes correlate very well.

5. Concluding remarks

The images of dendrites exhibit an interesting type of self-similarity. Firstly there is this system of thinning branches with repetitive branching sections. On the other hand due to its branches extending irregularly from a distinguished centre, one can analyse scaling of mass or other properties with central symmetry. Therefore special tools are needed to provide an adequate description of the structure and morphology of the dendrites. Fractal analysis offers several methods to address this problem, however not all of them are equally well handling it. Methods like IAM, IRRM or EABCM,

which take into account the geometric centre of the dendrite and analyse irregularities in the branches give an insight into iso/anisotropy of the cell structure. Others, like BCM, allow to investigate the branching (frequency, number of subbranches, thinning of the branches) rather than the aspects of symmetry.

PIFS-SF seems to be more sensitive than BCM, but in general, these two techniques are rather similar. They both reflect the visual complexity of the image and their results are well correlated with each other (see Table VIII). Moreover their results anticorrelate with electrophysiological responses of the cells. The values of correlation coefficient are, however, too low to state that the anticorrelation is meaningful.

More promising results are obtained for the first group of the fractal methods (IAM, IRRM, EABCM). It may suggest that the electrophysiological properties of amacrine cells depend more on the mass scaling and central symmetries (which are neglected by BCM and PIFS-SF) rather than branching and space-filling aspects. However, this conjecture needs further experimental and theoretical investigations.

We are very grateful to Prof. M.B.A. Djamgoz for helpful discussions and for providing us with the experimental data of amacrine cells from goldfish retina. We also greatly acknowledge the support of Silesian University of Technology grants BK-212/RCh4/01 and BK-256/RCH4/02.

REFERENCES

- [1] B. Alberts, D. Bray, J. Lewis, M. Raff, K. Roberts, J.D. Watson, *Molecular Biology of the Cell*, third ed., Garland Publ. Inc. New York, London 1994.
- [2] M. Hausser, N. Spruston, G.J. Stuart, *Science* **290**, 739 (2000).
- [3] M.B.A. Djamgoz, M. Krasowska, O. Martinoli, M. Sercano, S. Vallergera, Z.J. Grzywna, *J. Neurosci. Res.* **66**, 1208 (2001).
- [4] Z.J. Grzywna, M. Krasowska, L. Ostrowski, J. Stolarczyk, *Acta Phys. Pol. B* **32**, 1561 (2001).
- [5] Z.J. Grzywna, J. Stolarczyk, *Chaos, Solitons and Fractals* **13**, 897 (2002).
- [6] M.B.A. Djamgoz, Z.J. Grzywna, M. Krasowska, S. Vallergera, *Cell. Mol. Biol. Letters* **1**, 259 (1996).
- [7] H.F. Jelinek, G.N. Elston, *Fractals* **9**, 287 (2001).
- [8] G. Stuart, N. Spruston, M. Hausser, *Dendrites*, Oxford Univ. Press, 1999.
- [9] A.E. Jacquin, *IEEE Proc.*, **81**, No 10 (1993).
- [10] M. Barnsley, *Fractals Everywhere*, Academic Press Inc., 1988.
- [11] A. Lasota, J. Myjak, *Bulletin of the Polish Academy of Sciences, Mathematics*, **44**, No.1, (1996).